JACS
JOURNAL OF THE AMERICAN CHEMICAL SOCIETY
Article
pubs.acs.org/JACS

Nitrite and Hydroxylamine as Nitrogenase Substrates: Mechanistic Implications for the Pathway of N_2 Reduction

Sudipta Shaw,[†] Dmitriy Lukoyanov,[‡] Karamatullah Danyal,[†] Dennis R. Dean,[§] Brian M. Hoffman,*[,‡] and Lance C. Seefeldt*[,†]

[†]Department of Chemistry and Biochemistry, Utah State University, Logan, Utah 84322, United States
[‡]Department of Chemistry, Northwestern University, Evanston, Illinois 60208, United States
[§]Department of Biochemistry, Virginia Tech, 110 Fralin Hall, Blacksburg, Virginia 24061, United States

Supporting Information

ABSTRACT: Investigations of reduction of nitrite (NO_2^-) to ammonia (NH_3) by nitrogenase indicate a limiting stoichiometry, $NO_2^- + 6e^- + 12ATP + 7H^+ \rightarrow NH_3 + 2H_2O + 12ADP + 12P_i$. Two intermediates freeze-trapped during NO_2^- turnover by nitrogenase variants and investigated by Q-band ENDOR/ESEEM are identical to states, denoted ***H*** and ***I***, formed on the pathway of N_2 reduction. The proposed NO_2^- reduction intermediate hydroxylamine (NH_2OH) is a nitrogenase substrate for which the ***H*** and ***I*** reduction intermediates also can be trapped. Viewing N_2 and NO_2^- reductions in light of their common reduction intermediates and of NO_2^- reduction by multiheme cytochrome c nitrite reductase (ccNIR) leads us to propose that NO_2^- reduction by nitrogenase begins with the generation of NO_2H bound to a state in which the active-site FeMo-co (**M**) has accumulated two $[e^-/H^+]$ (E_2), stored as a (bridging) hydride and proton. Proton transfer to NO_2H and H_2O loss leaves **M**−$[NO^+]$; transfer of the E_2 hydride to the $[NO^+]$ directly to form HNO bound to FeMo-co is one of two alternative means for avoiding formation of a terminal **M**−[NO] thermodynamic "sink". The N_2 and NO_2^- reduction pathways converge upon reduction of NH_2NH_2 and NH_2OH bound states to form state ***H*** with $[-NH_2]$ bound to **M**. Final reduction converts ***H*** to ***I***, with NH_3 bound to **M**. The results presented here, combined with the parallels with ccNIR, support a N_2 fixation mechanism in which liberation of the first NH_3 occurs upon delivery of five $[e^-/H^+]$ to N_2, but a total of seven $[e^-/H^+]$ to FeMo-co when obligate H_2 evolution is considered, and not earlier in the reduction process.

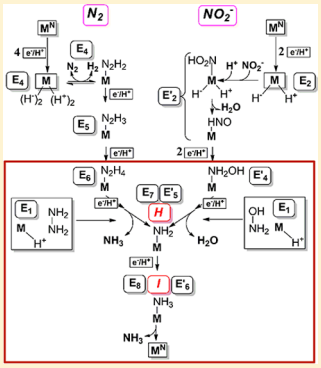

Nitrogenase, the metalloenzyme that catalyzes the reduction of dinitrogen (N_2) to two ammonia (NH_3) molecules, is the source of biologically fixed nitrogen within the biogeochemical N cycle.[1] The Mo-dependent nitrogenase comprises the MoFe protein, which contains the iron−molybdenum cofactor (FeMo-co) active site, and the Fe protein, which transfers electrons to the MoFe protein in a reaction coupled to the hydrolysis of MgATP.[2,3] In addition to "fixing" N_2, nitrogenase catalyzes the reduction of protons to form dihydrogen (H_2) and also catalyzes the reduction of a number of small, nonphysiological substrates.[2] Several of the nonphysiological substrates, and intermediates that form during their reduction by nitrogenase, have been extensively studied as probes of substrate interaction with FeMo-co.[2,4]

Alkyne substrates, such as acetylene (C_2H_2),[5] represent perhaps the best-characterized alternative nitrogenase substrates, but they react quite differently from N_2 in that they predominantly accept only two $[e^-/H^+]$ to form alkenes, whereas N_2 accepts six $[e^-/H^+]$ to form two NH_3, in a reaction that includes obligatory H_2 production.[6,7,4] Thus, N_2 reduction catalyzed by nitrogenase exhibits an optimal stoichiometry in which eight $[e^-/H^+]$ are consumed, eq 1.

$$N_2 + 8e^- + 16ATP + 8H^+ \rightarrow 2NH_3 + H_2 + 16ADP + 16P_i \quad (1)$$

The obligatory H_2 evolution, uniquely associated with N_2 binding, is reversible,[7,4] as evidenced by the observation that H_2 is a competitive inhibitor of N_2 reduction[8] and by the formation of $C_2DH_3/C_2H_2D_2$ during turnover under an atmosphere of $N_2/D_2/C_2H_2$.[4,9]

Nitrite (NO_2^-) was previously reported to be an alternative nitrogenous substrate for nitrogenase.[10] As a six-electron substrate that contains a single N atom and yields NH_3 as a reduction product, we surmised that it would be instructive to explore the catalytic pathway for NO_2^- reduction. Fundamental to the comparison of this pathway with that of N_2 reduction is whether NO_2^- reduction, like that of N_2, produces H_2 and thus obeys the eight $[e^-/H^+]$ stoichiometry of eq 1. Instead, it is shown here that NO_2^- reduction requires six $[e^-/H^+]$, together with an additional proton, to generate one NH_3 and two H_2O, eq 2

Received: July 14, 2014
Published: August 19, 2014

   dx.doi.org/10.1021/ja507123d | J. Am. Chem. Soc. 2014, 136, 12776−12783

$$NO_2^- + 6e^- + 12ATP + 7H^+ \rightarrow NH_3 + 2H_2O + 12ADP + 12P_i \quad (2)$$

a finding that implies distinct differences in the early stages of nitrogenase reduction of the two substrates.

The relationships between the full pathways for nitrogenase reduction of N_2 and NO_2^- have been addressed by freeze-quench trapping of intermediates formed during NO_2^- reduction using wild-type nitrogenase and remodeled nitrogenases having amino acid substitutions.[3,11] Intermediates trapped in this way have been characterized by Q-band ENDOR/ESEEM spectroscopies and compared to intermediates previously identified and characterized for N_2 reduction by the same approach.[7,4]

The finding that eq 2 describes NO_2^- reduction by nitrogenase also suggested the utility of comparisons with the six-electron reduction of this substrate by the multiheme enzyme cytochrome c nitrite reductase (ccNIR), whose catalytic mechanism has been deduced through the elegant studies by Neese, Einsle, and co-workers.[12−15] The identification of intermediates in NO_2^- reduction by nitrogenase revealed analogies with NO_2^- reduction by ccNIR that led to the prediction that hydroxylamine (NH_2OH), like N_2H_4,[7,4] would be a nitrogenase substrate, likewise reduced to NH_3. We therefore tested the capacity of nitrogenase to use NH_2OH as substrate, trapped and characterized NH_2OH reduction intermediates, and asked if H_2 is an inhibitor of NH_2OH reduction.

The findings of this study have implications for the pathway of N_2 fixation by nitrogenase that are derived from parallels with the pathways for NO_2^- reduction by nitrogenase and by ccNIR.

MATERIALS AND METHODS

Materials and Protein Purification. All reagents used were purchased from Sigma-Aldrich (St. Louis, MO), unless stated otherwise. ^{15}N sodium nitrite and hydroxylamine were purchased from Cambridge Isotope Laboratories, Inc. (Andover, MA). *Azotobacter vinelandii* strains DJ995 (wild-type MoFe protein), DJ884 (wild-type Fe protein), DJ1310 (MoFe protein α-70^{Val} residue substituted by Ala), and DJ1316 (α-70^{Val} residue substituted by Ala and α-195^{His} residue substituted by Gln) were grown, and nitrogenase proteins were expressed and purified as described.[16]

Proton, Dinitrogen, Nitrite, and Hydroxylamine Reduction Assays. Activity assays were performed in 1 mL liquid volumes in serum vials with 9 mL of total volume for various times at 30 °C in an assay buffer containing a MgATP and a regenerating system (5 mM ATP, 30 mM phosphocreatine, 100 mM MOPS, pH 7.0, 1.3 mg/mL bovine serum albumin, 0.2 mg/mL creatine phosphokinase, 6.7 mM $MgCl_2$, and 9 mM dithionite). Unless stated otherwise, reactions utilized 0.1 mg of MoFe protein, were initiated by the addition of 0.5 mg of Fe protein, and were quenched by the addition of 300 μL of 400 mM EDTA. H_2 was quantified by analyzing the gas phase by gas chromatography as previously described.[16] Nitrite and hydroxylamine reduction assays were carried out in the same buffer system except that 30 mM substrate was added before adding the proteins. Ammonia was quantified by a fluorescence method described before[17] with some modifications. A 25 μL aliquot of the postreaction solution was added to 1 mL of a solution containing 20 mM phthalic dicarboxyaldehyde, 3.5 mM 2-mercaptoethanol, 5% (v/v) ethanol, and 200 mM potassium phosphate, pH 7.3, and allowed to react in the dark for 30 min. Ammonia was detected by fluorescence ($\lambda_{excitation}/\lambda_{emission}$ of 410 nm/472 nm) and quantified by comparison to an NH_3 standard curve generated using NH_4Cl. The specific activities of the MoFe proteins were corrected on the basis of the concentration of Mo in each protein. The Mo content was determined using a colorimetric assay as described previously.[18]

EPR/ENDOR/ESEEM Spectroscopy. Variable-temperature X-band CW EPR spectra measurements were performed on a Bruker ESP 300 spectrometer equipped with an Oxford ESR 900 cryostat. Q-band ENDOR and ESEEM spectra were recorded at 2 K on CW[19] and pulsed[20,21] spectrometers. In both cases, the Q-band spectrum appears as the absorption envelope, rather than its derivative as in conventional EPR. The ENDOR response for an $I = {}^1/_2$ nucleus (^1H, ^{15}N) at a single orientation in a magnetic field presents a doublet centered at the nuclear Larmor frequency and split by the hyperfine coupling. The ReMims pulsed ENDOR sequence $[\pi/2-\tau_1-\pi/2-T(rf)-\pi/2-\tau_2-\pi-(\tau_1+\tau_2)-detect]$[22] was used in this work for detection of ^{15}N nuclei. This technique allows the use of short preparation interval τ_1 and broadens the range of hyperfine values that can be studied without distortions associated with the three pulse Mims ENDOR sequence.[23]

As in previous work,[24] in the three pulse ESEEM $[\pi/2-\tau-\pi/2-T-\pi/2-\tau-detect]$ sequence employed in this work for the study of non-Kramers ($S > 1$) centers,[25−27] the intensity of the echo is measured with varied T time at fixed τ, with appropriate phase-cycling to avoid unwanted features in the echo envelope. Spectral processing of time-domain waveforms includes subtraction of the relaxation decay fitted by a biexponential function, apodization with Hamming window, zero filling, and fast Fourier transformation performed with Bruker WIN-EPR software.

RESULTS

Nitrite and Hydroxylamine Reduction and Trapping. Vaughn and Burgess earlier demonstrated that nitrogenase reduces NO_2^- to yield NH_3 and two H_2O.[10] They assumed, without proof, that nitrogenase carries out this six-electron chemical process through the delivery of six electrons and seven protons to FeMo-co (eq 2). They further reported that NO_2^- inhibited proton reduction to H_2 catalyzed by nitrogenase via two mechanisms: inactivation of the Fe protein and by diversion of electron flow away from H_2 formation and toward NO_2^- reduction. Here, we examined the ability of the α-70^{Ala} and α-$70^{Ala}/\alpha$-195^{Gln} MoFe protein variants to reduce NO_2^-, comparing these results to those for wild-type MoFe protein. Substitution of α-70^{Val} by Ala in the MoFe protein has been shown to allow larger compounds to be substrates, and substitution of α-195^{His} by Gln has been shown to increase the population of trapped intermediates.[3,11,28]

As shown in Figure 1, wild-type and α-70^{Ala} MoFe proteins catalyze the reduction of N_2 or NO_2^- at comparable rates, consistent with rates reported previously for the wild-type enzyme.[10] It is notable that the α-70^{Ala} MoFe protein catalyzed the reduction of NO_2^- at rates significantly higher than the rate observed for N_2 reduction. In contrast, the α-$70^{Ala}/\alpha$-195^{Gln} MoFe protein shows a much lower rate of N_2 or NO_2^- reduction when compared to that of the wild-type or α-70^{Ala} protein. The doubly substituted protein also shows a higher rate of NO_2^- reduction compared to that of N_2 reduction.

Consistent with earlier reports,[8] H_2 was found to inhibit N_2 reduction in the wild-type MoFe protein (Figure 2A). This inhibition reflects the equilibrium between N_2 binding and H_2 release that is proposed to be associated with the reductive elimination of H_2 upon N_2 binding.[4] The release of H_2 leads to the enzymological requirement that eight electrons/protons be delivered to FeMo-co in order to achieve the six-electron reduction of N_2 to two NH_3, eq 1. The competitive binding of N_2/H_2 is an equilibrium process, so added H_2 competes with N_2 binding and inhibits NH_3 production. As seen in Figure 2A, H_2 also inhibits N_2 reduction in the α-70^{Ala} MoFe protein. Under these conditions of low N_2 partial pressure, the rates of

dx.doi.org/10.1021/ja507123d | J. Am. Chem. Soc. 2014, 136, 12776−12783

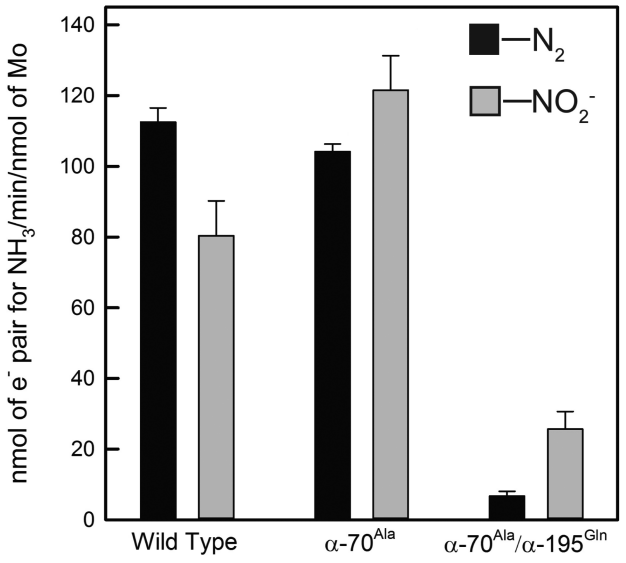

Figure 1. Reduction of N_2 and NO_2^- to NH_3 catalyzed by nitrogenase. The specific activity for electron pairs transferred to N_2 or NO_2^- is shown for wild-type, α-70^{Ala}, and α-$70^{Ala}/\alpha$-195^{Gln} MoFe proteins. Conditions: 1 atm for N_2 or 30 mM for NO_2^- at 30 °C. Specific activity was corrected to the Mo content in each protein.

N_2 reduction in the α-$70^{Ala}/\alpha$-195^{Gln} MoFe protein are below the detection limit. In contrast to these results, H_2 does not inhibit NO_2^- reduction for the wild-type or either of the two MoFe protein variants (Figure 2B). For these studies, a substrate concentration near the K_m for N_2 and NO_2^- was used, with H_2 between 0.8 and 1 atm. Similar studies were conducted at a lower NO_2^- concentration (0.8 mM versus 30 mM), with no observed inhibition by H_2 of ammonia formation (data not shown).

The absence of H_2 inhibition is interpreted as indicating that NO_2^- binding is not in equilibrium with H_2 release and that the six-electron reduction of NO_2^- indeed involves the delivery of six $[e^-/H^+]$ (plus an additional proton) to FeMo-co, as shown in eq 2.

NH_2OH has not previously been reported to be a substrate for nitrogenase. In Figure 3, it is shown that NH_2OH is a substrate for wild-type nitrogenase and is reduced to NH_3 at rates similar to the rates of N_2 reduction. In the α-70^{Ala} MoFe protein, the rate of reduction of NH_2OH is higher than the rates of N_2 reduction catalyzed by any of the proteins examined. In the α-$70^{Ala}/\alpha$-195^{Gln} MoFe protein, NH_2OH reduction rates were higher than N_2 reduction rates. Like nitrite, H_2 did not inhibit NH_2OH reduction rates.

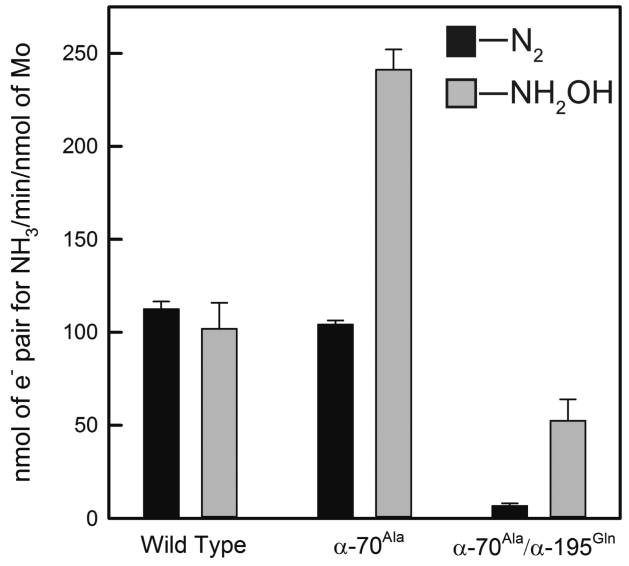

Figure 3. Reduction of N_2 and NH_2OH by nitrogenase. The specific activity for reduction of N_2 and NH_2OH to ammonia is shown for wild-type, α-70^{Ala}, and α-$70^{Ala}/\alpha$-195^{Gln} MoFe proteins. Conditions: 1 atm pressure of N_2 or 30 mM NH_2OH.

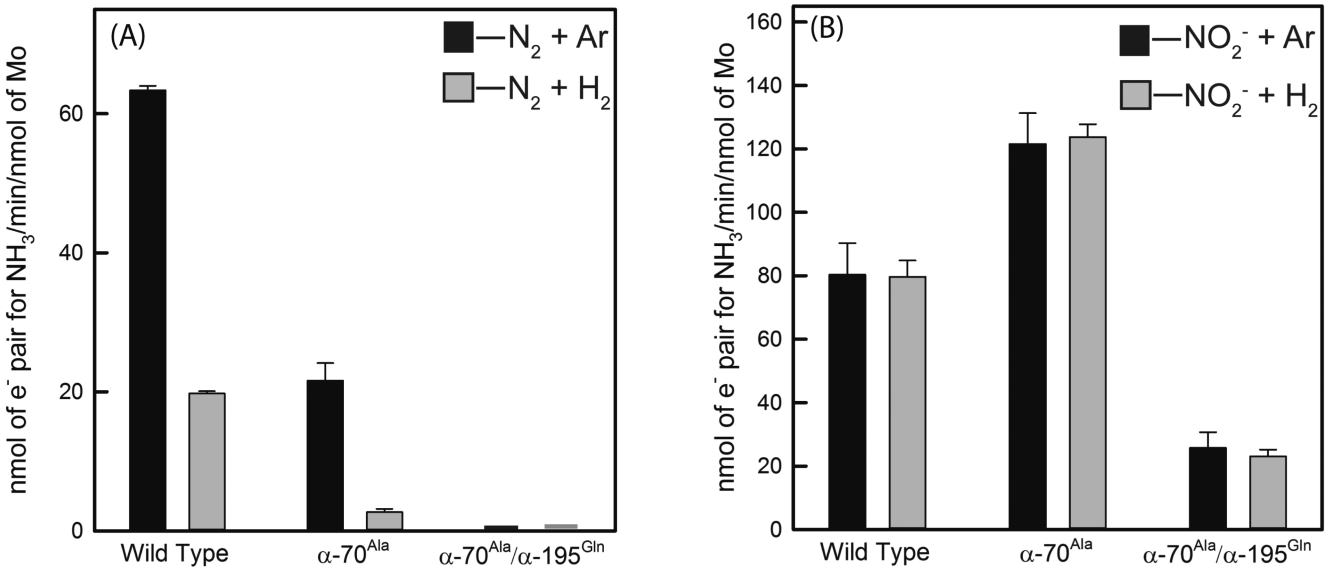

Figure 2. H_2 inhibition of N_2 and NO_2^- reduction. (A) H_2 inhibition of N_2 reduction in wild-type, α-70^{Ala}, and α-$70^{Ala}/\alpha$-195^{Gln} MoFe proteins. Conditions: 0.2 atm N_2 with 0.8 atm Ar (black) and 0.2 atm N_2 with 0.8 atm H_2 (gray). (B) Absence of H_2 inhibition of NO_2^- reduction in wild-type, α-70^{Ala}, and α-$70^{Ala}/\alpha$-195^{Gln}. Conditions: 1 atm argon (black) or 1 atm H_2 (gray) and 30 mM nitrite. Specific activity is corrected by the Mo content in the MoFe proteins. Substrate concentrations were selected near the established K_m values.

dx.doi.org/10.1021/ja507123d | J. Am. Chem. Soc. 2014, 136, 12776−12783

Characterization of Trapped States. Attempts to trap EPR-active intermediates during reduction of NO_2^- by the wild-type nitrogenase were not successful. In contrast, Q-band CW EPR spectra of the α-70^{Ala}/α-195^{Gln} MoFe protein treated with NO_2^- show small perturbations of the resting-state FeMo-co EPR signal ($S = {}^3/_2$). The absence of any ^{15}N ENDOR signals when $^{15}NO_2^-$ is added suggests that the substrate at most is weakly interacting with FeMo-co (data not shown).

EPR spectra of the α-70^{Ala}/α-195^{Gln} MoFe protein freeze-quenched during turnover in the presence of NO_2^- (Figure 4)

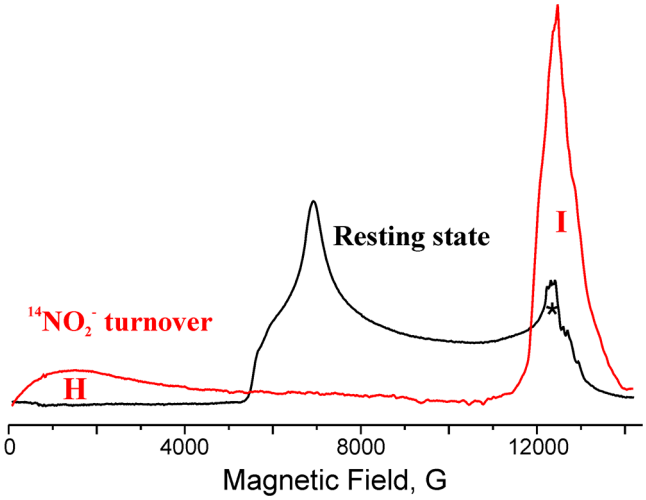

Figure 4. Absorption display Q-band CW EPR of α-70^{Ala}/α-195^{Gln} MoFe protein in the resting state (black) and trapped during turnover in the presence of nitrite (red). Conditions: microwave frequency, ~35.0 GHz; modulation amplitude, 1 G; time constant, 128 ms; field sweep, 67G/s; T = 2 K. The asterisk denotes a signal from traces of Mn^{2+}.

or NH_2OH (Figure S1) show complete loss of the resting-state signal and the appearance of signals from two EPR-active species: a broad integer-spin ($S \geq 2$) signal in low magnetic field and a narrow $S = {}^1/_2$ signal in high field. These spectra are similar to those of states ***H*** and ***I*** previously trapped during turnover of the α-70^{Ala}/α-195^{Gln} MoFe protein in the presence of hydrazine, diazene, or methyldiazene.[29,30] Those species were thoroughly studied by a variety of paramagnetic resonance spectroscopic methods and assigned as E_7 and E_8 states, respectively, of the Lowe−Thorneley (LT) kinetic scheme for N_2 fixation.[2]

As can be seen in Figure 5, the T = 4 K X-band EPR spectra of the $S = {}^1/_2$ states formed during NO_2^- and NH_2OH turnovers are identical to those of the ***I*** intermediate trapped during turnover of several N-substrates (e.g., N_2H_4). Measurements at other temperatures show that the spectra when NO_2^- or NH_2OH are used as substrates arise from two conformers, as previously observed for the ***I*** intermediate.[29] These conformers have slightly different g-tensors and exhibit very different relaxation properties: a fast-relaxing conformer with g_1 = 2.09, whose EPR could be observed unsaturated in X-band, T = 4 K (Figure 5), and a slowly relaxing conformer with g_1 = 2.10 is easily observable in X-band EPR spectra at higher temperatures and in CW Q-band spectra at lower temperatures.

The non-Kramers, $S \geq 2$, EPR signals seen in the low-field regions of Figures 4 and S1 are unresolved, as is true for the intermediate, ***H***, which forms on the pathway of N_2 reduction.[30] Such featureless spectra cannot be used to

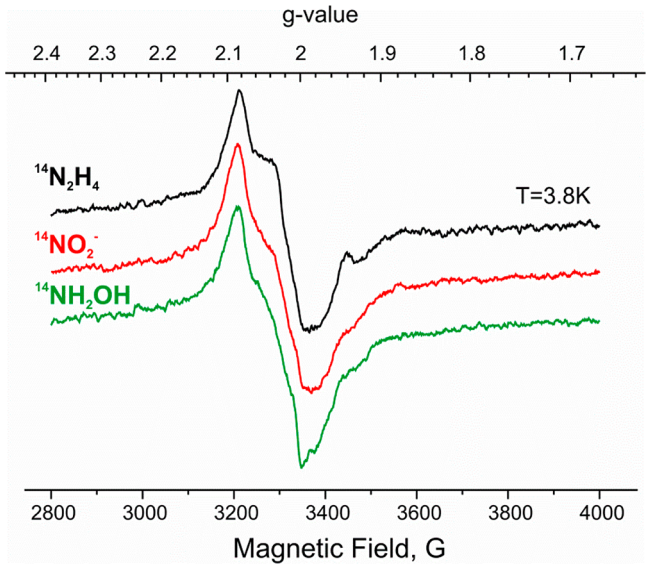

Figure 5. X-band EPR spectra of α-70^{Ala}/α-195^{Gln} MoFe protein turnover samples prepared with hydrazine (black), nitrite (red), and hydroxylamine (green) substrates. Conditions: microwave frequency, 9.36 GHz; microwave power, 10 mW; modulation amplitude, 7 G; time constant, 160 ms; field sweep, 20 G/s. Spectra are normalized to the same amplitude for comparison.

correlate the intermediates reported here for NO_2^- and hydroxylamine turnover with ***H***.

ENDOR/ESEEM Studies. CW ENDOR spectra of the $S = {}^1/_2$ NO_2^- and NH_2OH intermediates reveal the presence of protons that have a hyperfine coupling of ~7 MHz, Figure 6, in addition to signals from less strongly coupled protons. As shown, the full pattern is indistinguishable from that of ***I***, and, in particular, the 7 MHz signals are indistinguishable from those

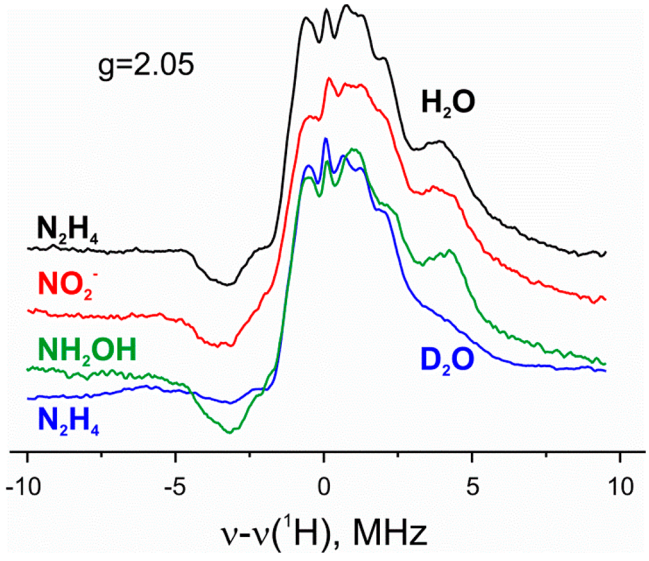

Figure 6. ^{1}H CW ENDOR spectra comparison of α-70^{Ala}/α-195^{Gln} MoFe protein hydrazine (black), nitrite (red), and hydroxylamine (green) turnover samples prepared in H_2O; included is a signal from a representative intermediate trapped during turnover in D_2O, formed with hydrazine substrate (blue). Conditions: microwave frequency, ~35.0 GHz; modulation amplitude, 2.5 G; time constant, 64 ms; bandwidth of RF broadened to 100 kHz; RF sweep, 1 MHz/s, 50−80 scans; T = 2 K.

dx.doi.org/10.1021/ja507123d | J. Am. Chem. Soc. 2014, 136, 12776−12783

of exchangeable protons of the ***I*** intermediate, which were assigned to an NH_3 derived from hydrazine bound to FeMo-co.

As illustrated in Figures 7 and S2, the ReMims ^{15}N Q-band ENDOR spectra taken at g ~ g_2 for $^{15}NO_2^-$ and $^{15}NH_2OH$

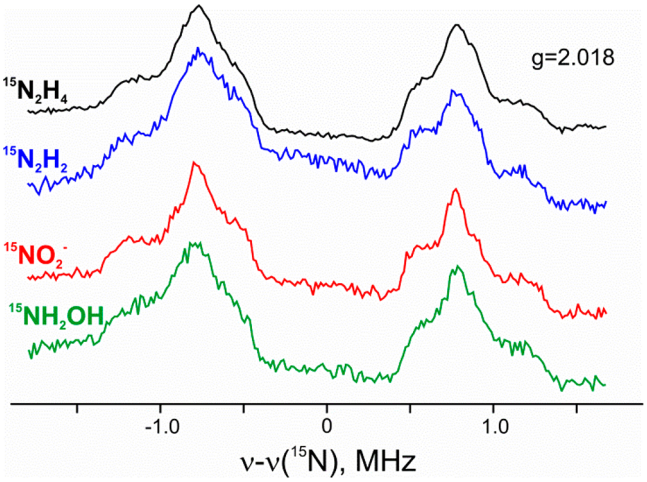

Figure 7. ReMims ^{15}N ENDOR spectra of $S = {}^1/_2$ intermediates trapped during turnover of α-$70^{Ala}/\alpha$-195^{Gln} MoFe protein in the presence of various ^{15}N labeled substrates: hydrazine (black), diazene (blue), nitrite (red), and hydroxylamine (green). Conditions: microwave frequency, ~34.8 GHz; ReMims sequence, $\pi/2$ = 30 ns, τ_1 = 200 ns; RF, 40 μs; repetition time, 10 ms (20 ms for hydroxylamine sample); 500−900 scans; T = 2 K.

turnover samples each show a hyperfine-split ^{15}N pattern centered at the ^{15}N Larmor frequency identical to that observed for the ***I*** intermediate trapped during turnover of ^{15}N labeled other nitrogenous substrates.[29] Spectra collected for the two new substrates at points along their EPR envelope likewise are identical to those of ***I*** (Figure S2), whose complete 2D field-frequency plot of ^{15}N spectra was simulated as arising from a single ^{15}N atom directly coordinated to FeMo-co with hyperfine tensor **A** = [1.0, 2.8, 1.5] MHz.

Taken together, the EPR, ^1H, and ^{15}N pulse ENDOR spectra of the $S = {}^1/_2$ intermediates of NO_2^- and NH_2OH turnover identify both of these species as being identical to the ***I*** intermediate previously seen for other nitrogenous substrates, assigned to the E_8 state in the LT scheme, which has ammonia product bound to FeMo-co. Thus, both the "N−N" nitrogenous substrates and the "N−O" substrates, NO_2^- and NH_2OH, give rise to ***I***, assigned as the E_8 state with NH_3 bound to FeMo-co.[7,4,29,30]

The non-Kramers (NK) state ***H*** trapped for the α-$70^{Ala}/\alpha$-195^{Gln} protein during reduction of hydrazine, diazene, and methyldiazene was assigned by means of Q-band ESEEM spectroscopy as an integer-spin state corresponding to the E_7 state of the LT scheme, formed subsequent to N−N bond cleavage and with an NH_2 fragment of substrate bound to FeMo-co.[30] We therefore carried out ESEEM measurements on the NK EPR signals trapped during NO_2^- and NH_2OH turnover, Figures 4 and S1, and compared the resulting spectra with those of intermediate ***H***. Figure 8 shows such spectra recorded at several low magnetic fields for the ***H*** intermediate trapped during turnover with ^{14}N and ^{15}N labeled diazene and the corresponding spectra for the NK species formed during turnover with ^{14}N and ^{15}N NO_2^- and NH_2OH. The difference in the time waves collected for the NK intermediates of ^{14}N and

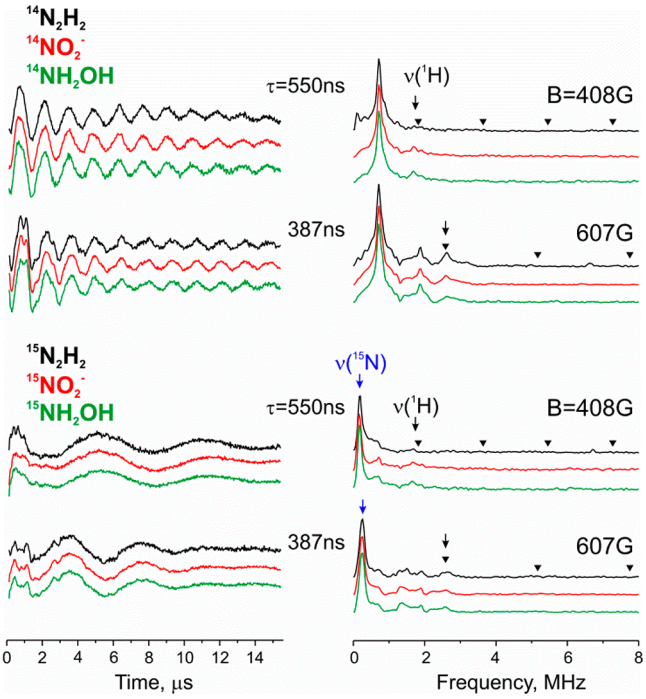

Figure 8. Q-band NK-ESEEM spectra in time (left) and frequency (right) domains obtained for integer-spin intermediates of α-$70^{Ala}/\alpha$-195^{Gln} MoFe protein turnover samples prepared with diazene (black), nitrite (red), and hydroxylamine (green). Upper spectra were measured for ^{14}N substrate samples, and lower spectra, for samples with ^{15}N labeled substrates. Conditions: microwave frequency, ~34.8 GHz; $\pi/2$ = 50 ns, 30 ns time steps; repetition time, 10 ms, 10 shots/point for diazene turnovers and 2 ms, 50 shots/point for other turnovers, 200−300 scans; T = 2 K. Time-waves are shown after decay baseline subtraction. Triangles in the frequency domain spectra represent suppressed frequencies n/τ, n = 1, 2, ...

^{15}N substrates clearly shows that the signals arise from FeMo-co that binds a reduction product of substrate. The identity of both ^{14}N and ^{15}N time waves and their partner frequency-domain spectra for the NO_2^- and NH_2OH intermediates with those of the ***H*** intermediate show that reduction of both these new substrates give rise to species ***H***.

DISCUSSION

The present study has extended the characterization of NO_2^- as a nitrogenase substrate previously reported by Vaughn and Burgess.[10] Here, it is established that the reduction of NO_2^- indeed involves the delivery of six electrons to FeMo-co, eq 2, rather than eight electrons as required for the reduction of N_2, eq 1. In addition, it has been shown that NH_2OH is an excellent nitrogenase substrate. The characterization of trapped intermediates during reduction of NO_2^- and NH_2OH catalyzed by remodeled nitrogenase MoFe protein provides insights into the mechanism for their reduction that also are relevant to the mechanism for N_2 reduction.

The Proposed Mechanism for N_2 Reduction. As a reference for discussing the mechanisms of NO_2^- and NH_2OH reduction by nitrogenase, Figure 9, left, displays a previously proposed pathway for N_2 reduction (alternating) by nitrogenase (**M** represents FeMo-co).[7,4] In this scheme, the six-electron reduction of N_2 to two NH_3 is accompanied by the obligatory loss of H_2 through reductive elimination upon N_2 binding, resulting in the stoichiometry of eq 1. Each catalytic

dx.doi.org/10.1021/ja507123d | J. Am. Chem. Soc. 2014, 136, 12776−12783

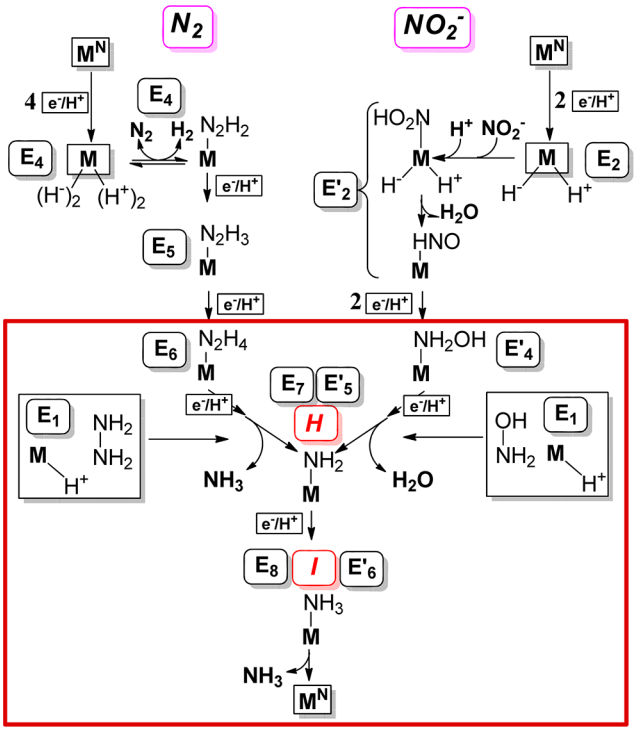

Figure 9. (Left) Previously proposed pathway for N_2 reduction by nitrogenase (**M** represents FeMo-co).[4] An intermediate, labeled E_n, has accumulated n [e^-/H^+]. (Right) Proposed dominant pathway for nitrite reduction by nitrogenase; intermediates of NO_2H reduction are labeled E'_m, with accumulation of m [e^-/H^+]. Early stages, through reduction to HNO, are shown in more detail in Figure 11. (Boxed Region) Convergence of pathways for nitrite and N_2 reduction by nitrogenase, as discussed in the text. Within this region, boxed reactions of E_1 show the most direct routes by which N_2H_4 and NH_2OH join their respective pathways.

stage in this pathway is denoted E_n following the Lowe and Thorneley kinetic model,[2] where n = 0–8 denotes the number of electron/protons delivered to FeMo-co by the Fe protein.

Stoichiometry and Pathway of Nitrogenase Reduction of NO_2^-. Our findings regarding the stoichiometry and early stages of NO_2^- reduction by nitrogenase are as follows. (i) Addition of NO_2^- to resting-state MoFe protein causes minimal change in its EPR spectrum and introduces no ENDOR signals from $^{15}NO_2^-$. This observation suggests that NO_2^- (or NO_2H) does not bind to a metal ion of FeMo-co in resting-state MoFe protein. (ii) Although the addition of H_2 to nitrogenase during N_2 reduction inhibits the formation of NH_3, such addition during NO_2^- reduction does not, Figure 2. This result indicates that the reversible loss of H_2 upon N_2 binding, Figure 9, left, leading to the eight-electron stoichiometry of eq 1, has no parallel in the reduction of NO_2^-. Instead, we suggest that the dominant pathway for NO_2^- reduction begins with binding at E_2 and that NO_2^- reduction is a true six-electron process that has the stoichiometry of eq 2, above.

Further insights into NO_2^- reduction by nitrogenase arise from comparison with the ccNIR mechanism, Figure 10.[12−15,31] NO_2^- binds to the ccNIR catalytic heme in the Fe^{2+} state, accepts two protons, and releases H_2O to form a moiety formally written as Fe(II)−[NO^+], denoted {FeNO}^{6} in the Enemark−Feltham notation.[32] The key mechanistic challenge in reducing NO_2^- is to avoid or overcome formation of the terminal Fe(II)−NO "thermodynamic sink", denoted as

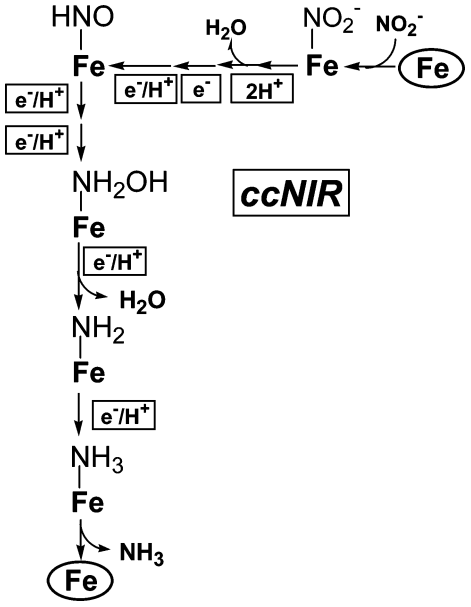

Figure 10. Mechanism of NO_2^- reduction by ccNIR; initial and final states contain Fe(II) heme.[12−15]

{FeNO},[7] through one-electron reduction of Fe(II)−[NO^+].[31] Neese and co-workers have shown that ccNIR achieves this by two proton-coupled electron transfer reductions that promptly reduce Fe(II)−[NO^+] to Fe(II)−[HNO].[12−15] The process involves "recharging" of the catalytic heme with electrons obtained through transfer from the other hemes of the enzyme and of the heme environment with protons.

The ability[4] of the multimetallic catalytic FeMo-co cluster to accumulate multiple [e^-/H^+] offers two persuasive alternative mechanisms by which nitrogenase can completely evade the formation of an intermediate with terminal NO bound to **M**, **M**−[NO], the analogue to {FeNO}.[7] As visualized in Figure 11, we suggest that NO_2^- reduction by nitrogenase begins with

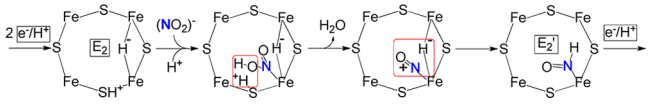

Figure 11. Proposed early stages of the reduction of NO_2^- by nitrogenase. The placement of proton and hydride on specific S and Fe atoms of E_2 is arbitrary.

the generation of NO_2H bound to E_2; whether NO_2^- accepts the proton before or after binding is unknown; likewise, whether NO_2^- also can bind to E_1, with this state accepting an [e^-/H^+] to form NO_2^--bound E_2, is not known. As illustrated, E_2 has accumulated two [e^-/H^+], stored in the form of a hydride bridging between two Fe atoms and a proton bound to sulfur. Transfer of the E_2 proton to the −OH of NO_2H followed by loss of H_2O formally leaves **M**−[NO^+], an analogue to the Fe(II)−[NO^+] state of ccNIR. However, nitrogenase is able to transfer the E_2 hydride to [NO^+], directly forming HNO bound to FeMo-co at its resting-state redox level and totally avoiding formation of an **M**−[NO] "sink". The reduction of [NO^+] by hydride transfer at the E_2 stage not only parallels our proposed mechanism for reduction of acetylene (C_2H_2) to ethylene (C_2H_4)[4,9] but also is analogous to the process by which P450nor reduces heme-bound NO to bound

dx.doi.org/10.1021/ja507123d | J. Am. Chem. Soc. 2014, 136, 12776−12783

HNO: direct hydride transfer from NADH.[33] There is a second mechanism by which FeMo-co might avoid the formation of an M−[NO] sink. The proximity of Fe ions might allow formation of a bridged NO, which would likely be reactive to addition of an $[e^-/H^+]$.[34]

Although the stages of NO_2^- reduction through the formation of HNO are thus proposed to differ for catalysis by nitrogenase and ccNIR, the ENDOR and ESEEM results presented here indicate that the subsequent reduction of FeMo-co-bound HNO follows the stages proposed by Neese and cowokers for ccNIR, which include formation of Fe-NH_2 and Fe-NH_3 intermediates that are analogues to intermediates ***H*** and ***I***, Figure 10. The resulting overall pathway for NO_2^- reduction by nitrogenase is presented on the right of Figure 9 for comparison to the pathway for N_2 reduction on the left. The NO_2^- intermediates that form by transfer of additional $[e^-/H^+]$ to the HNO-bound state are denoted E'_m, with the prime indicating the alternative substrate and the differing numbers of electrons delivered to FeMo-co (two fewer for NO_2^- than for N_2) required to achieve the same level of substrate reduction (eqs 1 and 2) in the intermediate.

Mechanistic Convergence and Its Implications. The overall stoichiometries and early stages of N_2 and NO_2^- reduction by nitrogenase differ sharply, with reductive elimination of H_2 being a central feature of N_2 fixation but absent for NO_2^- reduction or reduction of any other nitrogenase substrate studied so far. However, the ENDOR/ESEEM study of trapped intermediates indicates that the reaction pathways converge to corresponding intermediates, which then react to form the identical states ***H*** and ***I***, as captured in the boxed section of the two catalytic pathways, Figure 9.

The boxed portion of the NO_2^- pathway begins with an intermediate (denoted E'_4) that contains NH_2OH bound to FeMo-co (**M**), equivalent to the ccNIR intermediate, in which NH_2OH is bound to the catalytic heme (Figure 10). The nitrogenase NH_2OH intermediate corresponds to the E_6 stage of N_2 fixation in which N_2H_4, itself a substrate, is bound to **M**. The proposed formation of such corresponding NH_2NH_2- and NH_2OH-bound intermediates suggested to us that NH_2OH, like N_2H_4, should be a nitrogenase substrate. This prediction was verified by measurements that show NH_2OH is indeed an excellent substrate (Figure 3). The reduction of NH_2OH, like that of N_2H_4, is not inhibited by the presence of H_2, as expected for reaction of late-stage reduction intermediates.

The ENDOR/ESEEM measurements show that the pathways for N_2 and NO_2^- reduction converge upon reduction of the corresponding $E_6(NH_2NH_2)$ and $E'_4(NH_2OH)$ states (Figure 9). The two substrate-derived moieties of E_6/E'_4, N_2H_4/NH_2OH, may be viewed as $NH_2{-}AH_x$ species exhibiting an N−A single bond, A = N or O. The pathways converge through reductive cleavage of the N−A bond, liberating AH_m (m = 3 or 2) and formation of the common, non-Kramers state ***H*** with NH_2 bound to **M** (E_7 stage for N_2; E'_5 for NO_2^-). A final reduction then converts ***H*** to intermediate ***I*** (E_8 for N_2; E'_6 for NO_2^-), with NH_3 bound to **M**. The catalytic process is finally completed by the liberation of NH_3, as previously proposed for N_2 reduction by nitrogenase and for NO_2^- reduction by ccNIR. Figure 9 also shows the most direct route by which both N_2H_4 and NH_2OH, independently acting as substrates, join their respective reaction pathways: they bind to E_1 and undergo bond cleavage, respectively liberating NH_3 and H_2O and generating the ***H*** intermediate.

Given the findings that not only N_2H_4 (and N_2H_2) but also NH_2OH are excellent nitrogenase substrates and that common ***H*** and ***I*** intermediates form during nitrogenase turnover with both NO_2^- and NH_2OH on one hand and with dinitrogenous substrates N_2H_4 and N_2H_2 on the other, the present study supports proposals that (i) N_2H_4 and NH_2OH are indeed generated on the enzymatic pathways by which nitrogenase reduces the primary substrates, N_2 and NO_2^-; (ii) these results are consistent with an alternating pathway for nitrogen fixation in which the first NH_3 is generated by N−N bond cleavage upon delivery of the seventh $[e^-/H^+]$ to the E_6 (N_2H_4-bound) intermediate to form ***H*** = E_7 and the second NH_3 by delivery of the eighth and last $[e^-/H^+]$ to form ***I*** = E_8, Figure 9, left; (iii) NO_2^- reduction proceeds by the analogous and convergent pathway, in which the H_2O is liberated by reductive cleavage of the NH_2−OH-bound intermediate to form ***H*** = E'_5 and NH_3 is produced by delivery of the sixth and last $[e^-/H^+]$ ***I*** = E'_6, Figure 9, right.

According to the alternative Chatt−Schrock mechanism for N_2 fixation so beautifully demonstrated for mononuclear Mo complexes,[35−37] the N−A bond would be cleaved earlier in the reduction processes, after delivery of three $[e^-/H^+]$ to the substrate, at the E_5 stage for N_2 reduction and at the HNO stage for NO_2^- reduction (E'_3), to leave a bound nitride. As a result, neither the N_2H_4 nor the NH_2OH intermediates would likely form, making it unlikely that both of these species would be substrates. We further emphasize that application of this proposal to nitrogenase reduction of NO_2^- would be contrary to the mechanism established for NO_2^- reduction by ccNIR, which does not involve cleavage of the N−O bond to form a heme-bound nitride at the third step in substrate reduction, but cleavage at the fifth step to form NH_2.[12−15,31] Overall, the parallels between N_2 fixation by nitrogenase, NO_2^- and NH_2OH reduction by nitrogenase, and NO_2^- reduction by ccNIR support the parallel nitrogenase pathways presented in Figure 9, with N−A bond cleavage after delivery of the fifth $[e^-/H^+]$ to substrate, to yield the **M**−NH_2, ***H*** intermediate.

Namely, while we have not yet trapped and characterized the E_5 and E_6 intermediates, the current report supports a mechanism in which N−N bond cleavage and liberation of the first NH_3 occurs during formation of the E_7 intermediate (delivery of five $[e^-/H^+]$ to substrate), ***H***, and not earlier in the reduction process, through bond cleavage at E_5 (delivery of three $[e^-/H^+]$ to substrate) with formation of a nitrido-bound intermediate.

■ ASSOCIATED CONTENT

Supporting Information

Q-band CW EPR and ReMims ENDOR data. This material is available free of charge via the Internet at http://pubs.acs.org.

■ AUTHOR INFORMATION

Corresponding Authors

bmh@northwestern.edu
lance.seefeldt@usu.edu

Notes

The authors declare no competing financial interest.

■ ACKNOWLEDGMENTS

This work was supported by grants from the NIH (GM 111097 to B.M.H.), the DOE (DE-SC0010687 to L.C.S. and D.R.D.), and the NSF (MCB 1118613 to B.M.H.).

REFERENCES

(1) Smil, V. *Enriching the Earth: Fritz Haber, Carl Bosch, and the Transformation of World Food Production*; The MIT Press: Cambridge, MA, 2004.
(2) Burgess, B. K.; Lowe, D. J. *Chem. Rev.* **1996**, *96*, 2983.
(3) Seefeldt, L. C.; Hoffman, B. M.; Dean, D. R. *Annu. Rev. Biochem.* **2009**, *78*, 701.
(4) Hoffman, B. M.; Lukoyanov, D.; Yang, Z.-Y.; Dean, D. R.; Seefeldt, L. C. *Chem. Rev.* **2014**, *114*, 4041.
(5) Dilworth, M. J. *Biochim. Biophys. Acta* **1966**, *127*, 285.
(6) Simpson, F. B.; Burris, R. H. *Science* **1984**, *224*, 1095.
(7) Hoffman, B. M.; Lukoyanov, D.; Dean, D. R.; Seefeldt, L. C. *Acc. Chem. Res.* **2013**, *46*, 587.
(8) Guth, J. H.; Burris, R. H. *Biochemistry* **1983**, *22*, 5111.
(9) Yang, Z.-Y.; Khadka, N.; Lukoyanov, D.; Hoffman, B. M.; Dean, D. R.; Seefeldt, L. C. *Proc. Natl. Acad. Sci. U.S.A.* **2013**, *110*, 16327.
(10) Vaughn, S. A.; Burgess, B. K. *Biochemistry* **1989**, *28*, 419.
(11) Dos Santos, P. C.; Igarashi, R. Y.; Lee, H.-I.; Hoffman, B. M.; Seefeldt, L. C.; Dean, D. R. *Acc. Chem. Res.* **2005**, *38*, 208.
(12) Einsle, O.; Messerschmidt, A.; Huber, R.; Kroneck, P. M. H.; Neese, F. *J. Am. Chem. Soc.* **2002**, *124*, 11737.
(13) Bykov, D.; Plog, M.; Neese, F. *J. Biol. Inorg. Chem.* **2014**, *19*, 97.
(14) Bykov, D.; Neese, F. *J. Biol. Inorg. Chem.* **2012**, *17*, 741.
(15) Bykov, D.; Neese, F. *J. Biol. Inorg. Chem.* **2011**, *16*, 417.
(16) Christiansen, J.; Cash, V. L.; Seefeldt, L. C.; Dean, D. R. *J. Biol. Chem.* **2000**, *275*, 11459.
(17) Barney, B. M.; Laryukhin, M.; Igarashi, R. Y.; Lee, H.-I.; Dos Santos, P. C.; Yang, T.-C.; Hoffman, B. M.; Dean, D. R.; Seefeldt, L. C. *Biochemistry* **2005**, *44*, 8030.
(18) Barney, B. M.; Yurth, M. G.; Santos, P. C. D.; Dean, D. R.; Seefeldt, L. C. *J. Biol. Inorg. Chem.* **2009**, *14*, 1015.
(19) Werst, M. M.; Davoust, C. E.; Hoffman, B. M. *J. Am. Chem. Soc.* **1991**, *113*, 1533.
(20) Davoust, C. E.; Doan, P. E.; Hoffman, B. M. *J. Magn. Reson., Ser. A* **1996**, *119*, 38.
(21) Zipse, H.; Artin, E.; Wnuk, S.; Lohman, G. J. S.; Martino, D.; Griffin, R. G.; Kacprzak, S.; Kaupp, M.; Hoffman, B.; Bennati, M.; Stubbe, J.; Lees, N. *J. Am. Chem. Soc.* **2009**, *131*, 200.
(22) Doan, P. E.; Hoffman, B. M. *Chem. Phys. Lett.* **1997**, *269*, 208.
(23) Schweiger, A.; Jeschke, G. *Principles of Pulse Electron Paramagnetic Resonance*; Oxford University Press: Oxford, UK, 2001.
(24) Lukoyanov, D.; Barney, B. M.; Dean, D. R.; Seefeldt, L. C.; Hoffman, B. M. *Proc. Natl. Acad. Sci. U.S.A.* **2007**, *104*, 1451.
(25) Hoffman, B. M. *J. Phys. Chem.* **1994**, *98*, 11657.
(26) Hoffman, B. M.; Sturgeon, B. E.; Doan, P. E.; DeRose, V. J.; Liu, K. E.; Lippard, S. J. *J. Am. Chem. Soc.* **1994**, *116*, 6023.
(27) Sturgeon, B. E.; Doan, P. E.; Liu, K. E.; Burdi, D.; Tong, W. H.; Nocek, J. M.; Gupta, N.; Stubbe, J.; Kurtz, D. M.; Lippard, S. J.; Hoffman, B. M. *J. Am. Chem. Soc.* **1997**, *119*, 375.
(28) Dos Santos, P. C.; Mayer, S. M.; Barney, B. M.; Seefeldt, L. C.; Dean, D. R. *J. Inorg. Biochem.* **2007**, *101*, 1642.
(29) Lukoyanov, D.; Dikanov, S. A.; Yang, Z.-Y.; Barney, B. M.; Samoilova, R. I.; Narasimhulu, K. V.; Dean, D. R.; Seefeldt, L. C.; Hoffman, B. M. *J. Am. Chem. Soc.* **2011**, *133*, 11655.
(30) Lukoyanov, D.; Yang, Z.-Y.; Barney, B. M.; Dean, D. R.; Seefeldt, L. C.; Hoffman, B. M. *Proc. Natl. Acad. Sci. U.S.A.* **2012**, *109*, 5583.
(31) Maia, L. B.; Moura, J. J. G. *Chem. Rev.* **2014**, *114*, 5273.
(32) Enemark, J. H.; Feltham, R. D. *Coord. Chem. Rev.* **1974**, *13*, 339.
(33) Riplinger, C.; Neese, F. *ChemPhysChem* **2011**, *12*, 3192.
(34) García, M. E.; Melón, S.; Ruiz, M. A.; Marchiò, L.; Tiripicchio, A. *J. Organomet. Chem.* **2011**, *696*, 559.
(35) Schrock, R. R. *Proc. Natl. Acad. Sci. U.S.A.* **2006**, *103*, 17087.
(36) Weare, W. W.; Dai, X.; Byrnes, M. J.; Chin, J. M.; Schrock, R. R.; Müller, P. *Proc. Natl. Acad. Sci. U.S.A* **2006**, *103*, 17099.
(37) Yandulov, D. V.; Schrock, R. R. *Science* **2003**, *301*, 76.